Effect of the Mullins softening on mode I fracture of carbon-black filled rubbers

Julie Diani* Mathias Brieu Katharina Batzler Pierre Zerlauth

Abstract

The effect of the Mullins softening on mode I fracture of carbon-black filled rubbers was investigated experimentally. Large specimen of NR and SBR filled with the same amount and nature of carbon-black were submitted to uniaxial tension. Then, single edge notch tension samples were cut along various directions with respect to the direction of preconditioning, and submitted to tension until break. The fracture energy was estimated and compared according to the intensity of Mullins softening already undergone in the direction of crack opening and according to the softening undergone in other directions. The NR shows significantly improved resistance to crack propagation compared to the SBR due to its crystallization ability. For both materials, it was observed that a moderate prestrain has a positive impact increasing the material fracture toughness and that material softening and anisotropy induced by Mullins effect does not show on resistance to mode I crack propagation.

Mullins effect filled rubbers Tearing energy crack opening

1 Introduction

Crack propagation in tires is usually studied in fatigue, submitting rubbers to moderate strain cyclic loadings during a large number of cycles (Cadwell et al. 1940, Mars and Fatemi 2002). Nonetheless, for civil engineering applications, tires may sustain severe strain conditions and critical crack propagation may be observed within very few cycles. Therefore, understanding the resistance to crack growth during monotonous loadings is of interest for the latter applications. The objective of the current contribution is to study the possible impact of large prestrains on the resistance to mode I crack propagation in carbon-black filled rubbers.

A natural rubber (NR) and a styrene butadiene rubber (SBR) filled with the same amount and same type of carbon-black are considered. Strain induced crystallization in filled natural rubber is known to retard crack growth, increasing significantly the critical energy release rate compared to non-crystallizing filled gum like SBR (Buist 1945, Hamed 2005, Gherib et al. 2010 among others). What remains to be explored is how Mullins softening (Mullins 1969, Diani et al. 2009), exhibited by carbon-black filled rubbers, affects the resistance to crack propagation. The Mullins effect experienced by filled rubbers when first stretched above the maximum stretch ever applied, induces anisotropic softening (Diani et al. 2006, Itskov et al. 2006, Machado et al. 2012 for instance) which consequences on the resistance to crack propagation remains unknown. Since the anisotropic softening may be characterized by a three-dimensional envelope that has been assessed on experimental evidences (Merckel et al. 2012), it is relevant to study not only the impact of the softening magnitude but also its directional aspect on crack propagation. Therefore, large samples of filled NR and filled SBR are uniaxial stretched, then smaller samples cut at

*julie.diani@ensam.eu

0, 45 and 90 degrees with respect to the prestretch tensile direction are submitted to single notch crack propagation in mode I. This experimental work will allow us estimating the critical energy release rate for a crystallizing gum and a non-crystallizing gum according to the Mullins softening suffered by the material.

2 Theory

2.1 Critical energy release rate G_c

Rubbers are brittle and the Griffith's fracture criterion ($G \geq G_c$) applies (Griffith 1921). The propagation of a crack depends on the critical strain energy release rate G_c corresponding to the energy per unit area required to open the crack. Considering a single edge notch tensile (SENT) sample, as long as the initial length of the crack is small compared to the other dimensions of the sample, the energy release rate G may be calculated according to the expression established by Rivlin and Thomas (1953):

$$G = 2aKU \tag{1}$$

where U is the stored elastic energy density, a is the initial crack length and K is a function dependent of the macroscopic stretch λ applied to the sample. Lake (1970) proposed an expression of $K = \frac{\pi}{\sqrt{\lambda}}$ that was later simplified by Lindley (1972) to $K = \frac{3}{\sqrt{\lambda}}$. Therefore the fracture energy G_c writes as:

$$G_c = \frac{6aU_c}{\sqrt{\lambda_{break}}} \tag{2}$$

with U_c the elastic energy density stored at crack propagation and λ_{break} the macroscopic stretch at break. Figure 1 illustrates how U_c and $\lambda_{break} = 1 + \epsilon_{break}$ are determined using the macroscopic stress-strain response recorded during the SENT test.

2.2 Mullins softening envelope

A Mullins effect criterion was defined by Merckel et al. (2012) as follows. Considering any direction of space, $\vec{u}$, characterized by its polar angle (θ, φ), the Mullins softening is activated when:

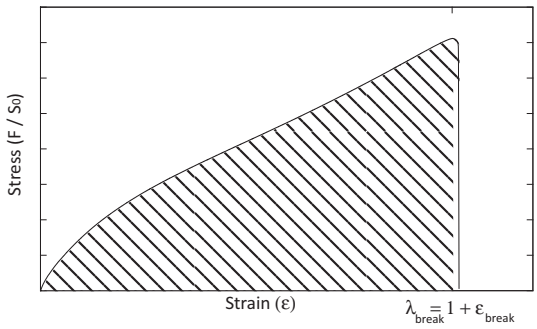

Figure 1: Typical stress-strain curve recorded during SENT test providing access to the measure of the critical elastic energy density stored U_c (hatched area) and to the stretch at break $\lambda_{break} = 1 + \epsilon_{break}$.

$$\exists \vec{u}(\theta, \varphi) \mid \lambda(\vec{u}) - \lambda_{max}(\vec{u}) = 0 \tag{3}$$

with $\lambda(\vec{u})$ defining the stretch according to direction $\vec{u}$, which maximum over the all loading history, $\max_{0 \to t}[\lambda(\vec{u})]$, is denoted $\lambda_{max}(\vec{u})$.

When submitting rubbers to a uniaxial tension up to stretch λ_M in direction $\vec{e}_1$, the Mullins threshold in any direction $\vec{u}$ in the stress-free sample plane may be easily estimated as:

$$\lambda_{max}(\vec{u}) = max\left(1, \sqrt{\lambda_M^2 u_1^2 + \frac{u_2^2}{\lambda_M}}\right) \tag{4}$$

with $u_1 = \vec{u}.\vec{e}_1$, $u_2 = \vec{u}.\vec{e}_2$, $\vec{e}_2$ being a vector in the stress-free sample plane such as $\vec{e}_1.\vec{e}_2 = 0$. Directions $\vec{u}$ may also be characterized by the angle θ between $\vec{e}_1$ and $\vec{u}$, then Figure 2 shows the Mullins softening threshold with respect to θ for various maximum stretches λ_M.

3 Materials and experiments

A styrene butadiene rubber (SBR) and a natural rubber (NR), both filled with 50 phr of N347 carbon

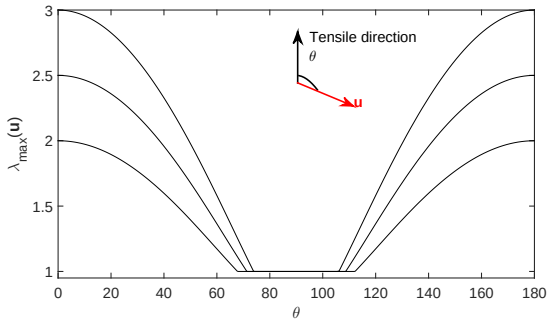

Figure 2: Mullins threshold envelopes in the stress-free sample plane according to the maximum stretch ($\lambda_M \in \{2, 2.5, 3\}$) uniaxially applied in direction characterized by the angle $\theta = 0$.

black, were manufactured by Michelin. Final products are rectangular plates of dimensions 150 x 150 x 2.5 mm^3. When stretched, the NR undergoes strain induced crystallization, increasing its strength and toughness, whereas the SBR does not crystallize.

Mechanical tests were performed on an Instron 5882 uniaxial tensile machine. The tensile force was measured by a 2 kN load cell. When uniaxial tension tests were run to characterize the Mullins softening or to apply a prestretch, uniaxial local strain was measured by video extensometry. For SENT tests, the macroscopic strain was monitored by recording the crosshead displacement only.

Prestretch uniaxial tension was applied on large specimen in order to possibly punch smaller samples for SENT tests that have been submitted to homogeneous states of strain. The homogeneity of the uniaxial prestrain was validated by evaluating the local deformation gradient tensor on the surface of a sample. For this purpose several dots were painted randomly on the sample surface (Figure 3a), which displacements were followed during the applied loading. The deformation gradient is calculated along the axes of the triangles displayed in Figure 3b). Figure 3c) and 3d) show the uniaxial and transverse stretches measured on the stress-free sample surface. As it can be seen in these figures, a large enough area of the sample is submitted to homogeneous strain, providing enough material to punch samples for SENT tests that have undergone homogeneous preloading.

SENT samples are 12 mm wide and 40 mm long. They are cut out from virgin plates or prestrained specimen at 0, 45 and 90 degrees with respect to the direction of prestretching. The notch is made with a razor blade and its length is measured with a microscope. The initial crack length, a, varied between 600 and 2200 μm. SENT samples were submitted to uniaxial tension until break with a constant crosshead speed of 5 mm/min. Since the elastic energy stored U_c corresponds to the tension force resulting work, the crosshead displacement is sufficient to calculate the critical energy release rate G_c (Eq. 2) and no local strain measurement is required. As for λ_{break} two options are possible. One may use the crosshead displacement at break to calculate the macroscopic stretch at break. This method is usually applied but is not necessarily very precise due to the large strain applied. Another option is to consider the local strain that would undergo a similar rectangular sample without a notch for the same macroscopic strain. We chose the latter one, but actually, it was noticed that choosing one or another method to estimate λ_{break} may change the absolute values of G_c but does not change the trends that are discussed in the result section.

Table 1 presents the various SENT tests run and their designations as SxAy, with x the applied uniaxial prestrain in % and y the angle along which the sample was cut after the preloading, 0 being the direction of prestrain.

Finally, let us note that when first loaded, filled rubbers may exhibit some residual strain that may need to be taken into account when computing the strain at the next loading (for instance when comparison are made with a virgin material). In this study, the maximum applied prestrain was 250%, and the residual strains were small enough to change the values of the critical energy release rate of about 2% only when taken into account. Therefore for simplicity reasons, the residual strain was neglected.

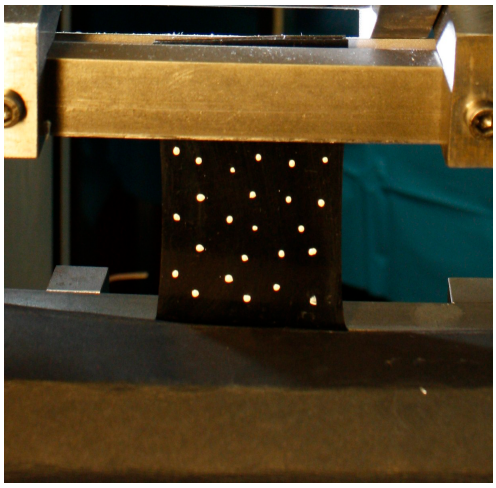

(a) Material submitted to a uniaxial prestrain

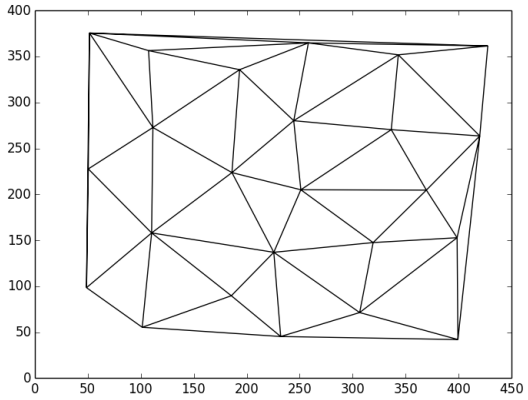

(b) Triangulation of specimen surface

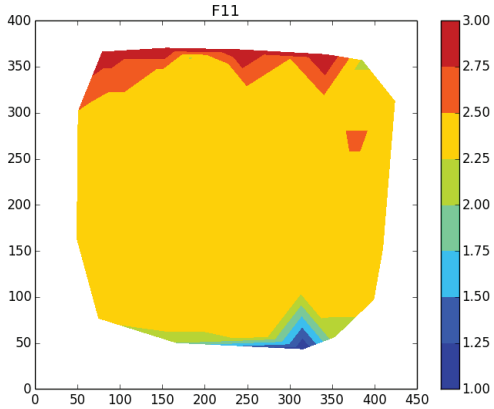

(c) Local values of uniaxial stretching

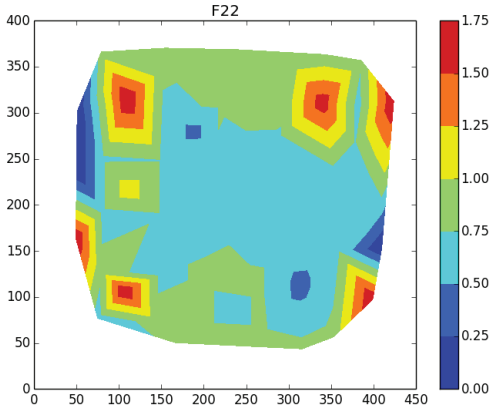

(d) Local values of stretching in the transverse direction

Figure 3: Uniaxial tension preloading applied on large samples. Validation of the homogeneous state of strain where the SENT sample are cut after the loading.

	Angle (°)		
prestrain %	0	45	90
0	S0A0	S0A45	S0A90
80	S80A0		
120	S120A0		
200	S200A0	S200A45	S200A90
250	S250A0		

Table 1: Designation of SENT tests that were run.

4 Results

4.1 Evidence of Mullins induced anisotropic softening

The initial in-plate isotropy of the materials was validated by punching three samples at 0, 45 and 90 degrees and comparing their responses in uniaxial tension. Then, large samples were submitted to uniaxial stretching up to 200% and specimen were cut at 0, 45 or 90 degrees with respect to the direction of prestrain to evidence the anisotropic Mullins softening. Figure 4 presents the stress-strain responses of the virgin material and of the prestrained samples according to the direction of cut. After being prestrained, the rubbers evidence stress-strain responses that are dependent of the direction of stretching. While specimens cut in the direction of prestraining display substantial softening, specimens cut at 45° present less softening and specimens cut at 90° show no softening at all. Note that for the NR, the crystallizing property of the material is known to be unaffected by the Mullins softening (Trabelsi et al., 2003). Such results are commonly known (Diani et al., 2009) but the impact of the Mullins softening and the induced anisotropy on the material resistance to crack opening remains to be explored.

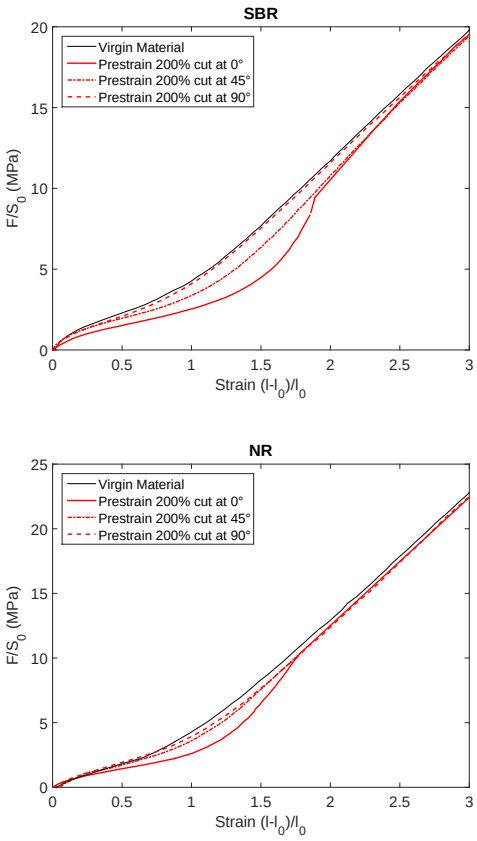

Figure 4: Material uniaxial stress-strain responses according to the direction of stretching after a uniaxial prestrain to 200% in direction 0°.

4.2 Effect of the Mullins softening intensity on crack propagation

For examining the effect of the magnitude of the Mullins softening, SENT tests are run in the same direction as the uniaxial prestrain. Specimens were submitted to uniaxial prestraining up to 0%, 80%,

120%, 200% or 250%, and SENT specimen were cut and loaded in the same direction as the prestrain. This refers to tests S0A0, S80A0, S120A0, S200A0 and S250A0 in Table 1. Figure 5 presents the average of critical energy release rate and twice its standard deviation obtained after running ten tests by experiments. One may notice the large error bars displayed by the standard deviation, which are classic for such tests and such materials and which expresses the need to run a large number of tests to approach a reasonable estimate of the average value of the strain energy release rate. As expected, NR exhibits a significantly larger energy at break than SBR. As mentioned before, this is due to its crystallizing property which delays the crack propagation. Crystallization is also responsible for crack deviation at the beginning of its propagation. As it can be seen in Figure 6, for NR the crack starts to propagates in the direction of stretching due to the presence of crystallites impeding the crack horizontal propagation. For both materials, once the crack propagates horizontally, the fracture is sudden and brittle producing smooth crack surfaces.

One reads in Figure 5 that submitting the rubbers to a moderate prestrain improves their resistance to crack opening. This might be due to the possible reorganization of the carbon-black microstructure when first stretch. Nonetheless, the increase in the strain energy release rate at moderate prestraining is more obvious for the SBR than for the NR. For the larger prestrains (200% and 250%), the critical energy release rate G_c returns to similar values as its value measured on the virgin material. It is also interesting to note that strains at failure measured during SENT tests increase with the preconditioning (Figure 7). The recorded values may be compared to the strains at break displayed by virgin unotched samples that average 2.6 for the SBR and 3.1 for the NR, the latter values being obtained over five uniaxial tension tests. Note that the strain at break of unotched samples tends also to increase when samples are prestretched as for instance in the case of a cyclic test with increasing maximum stretch.

Since the Mullins softening induces some anisotropy, the impact of a uniaxial prestrain on mode I crack opening in other directions than the direction of prestrain is evaluated in the next

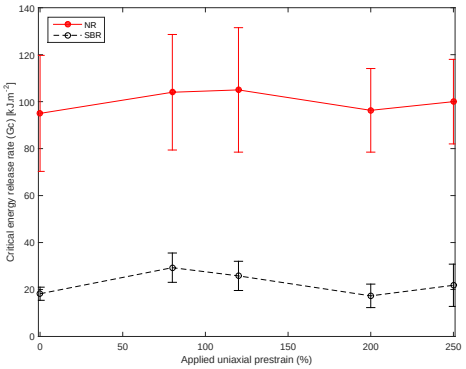

Figure 5: Measured critical energy release rate in mode I according to the uniaxial strain applied during the preconditioning.

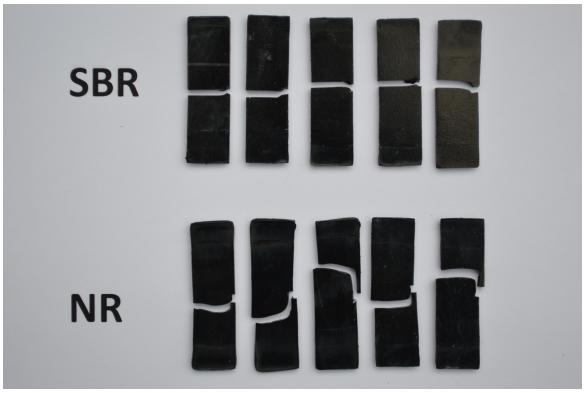

Figure 6: Illustration of the crack path during mode I propagation of SENT samples, the initial notch being always on the right of the samples.

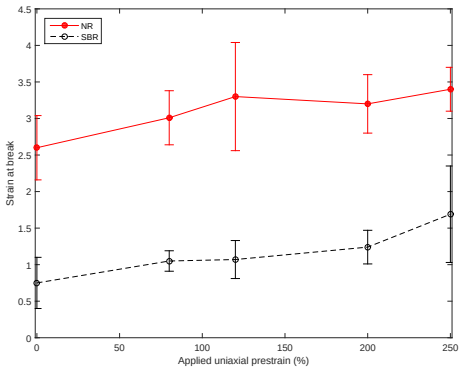

Figure 7: Strain at break of notched samples according to the uniaxial strain applied during the preconditioning.

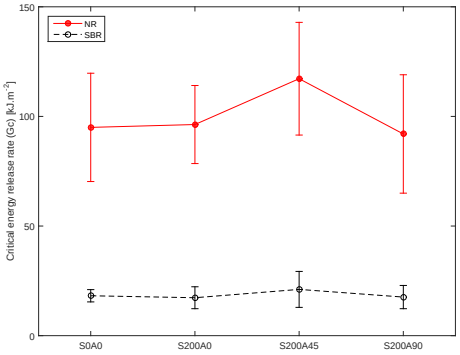

Figure 8: Average values and standard deviation of the critical energy release rate G_c according to the direction of SENT tests for material prestrained at 200% in direction 0°.

section.

4.3 Effect of the directional softening on crack propagation

Large specimen were submitted to uniaxial prestrain up to 200% and smaller SENT specimens are cut at 0, 45 and 90 degrees, in order to evaluate the impact of the uneven directional softening created by the prestrain. These tests are referenced S200A0, S200A45 and S200A90 in table 1. Figure 8 displays the values of the strain energy release rates measured according to the test considered. The case of the virgin material is also displayed for reference purpose. Note that the maximum strain undergone during the preconditioning, in the direction of tension of the SENT samples is different for each test. The comparison between the results from tests S0A0 and S200A0 has been discussed in the previous section. One notes that the strain energy release rate measured at 45° is above the reference value for S0A0. This may be explained by the fact that direction 45° was submitted to a strain of approximately 120% when the material was prestrained at 200% in direction 0° (see Figure 2). It was shown in Figure 5 that a prestrain of 120% in the direction of tension of the SENT specimens has a favorable impact on the critical energy release rate. In Figure 8, one reads that SENT samples cut at 90° with respect to the direction of prestrain exhibit mean value of G_c similar to the value obtain on virgin samples (S0A0). Note that the 90° direction does not undergo any softening during prestraining (Figure 4). This would mean that damage in other directions than the direction of crack opening has not a significant impact on G_c for the SBR as for the NR. The average strain at break measured during SENT tests S200A0, S200A45 and S200A90 are shown in Figure 9. Strain at break increases with the maximum strain applied in the direction of stretching, which is in agreement with measures plotted in Figure 7.

In order to further investigate the dependence of G_c to the damage already applied in other directions than the crack opening direction, values of G_c are compared for SENT samples that have been submitted to the same level of prestrain in the direction of the applied tension but various prestrain levels in other directions, i.e. tests S120A0 and S200A45. For both tests, the prestrain reached 120% in the direction of the SENT sample loading. Figure 10 shows the values of G_c measured during the SENT tests and their average values. For the SBR, G_c is similar for samples S200A45 and samples S0120, which is in favor of a negligible effect of the damage in other di-

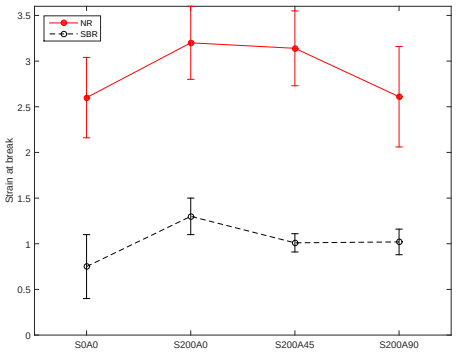

Figure 9: Strain at break of notched samples according to the direction of SENT tests for material prestrained at 200% in direction 0°.

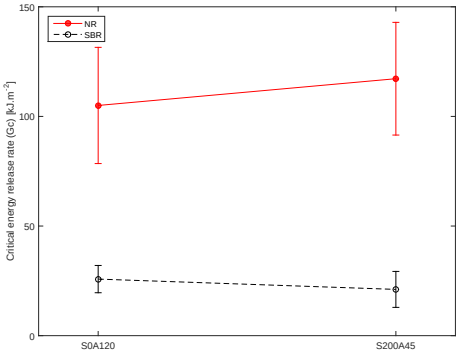

Figure 10: Average values and standard deviation of the critical energy release rate for SENT samples submitted to different preloading histories S120A0 and S200A45 (table 1) resulting in the same uniaxial prestrain of 120% in the direction of crack opening.

rections than the direction of crack opening. For the NR, the values of G_c measured during tests S200A45 are larger but the difference is not significant enough to recognize a real trend.

5 Conclusion

The impact of the Mullins softening on carbon-black filled rubber resistance to mode I crack propagation during monotonous loading was studied experimentally. For this purpose, a NR and a SBR filled with carbon-black were submitted to uniaxial preconditioning and SENT samples were cut in various directions in order to study the consequences of damage induced by the Mullins softening. Due to its crystallizing ability, NR demonstrates significantly larger resistance to tear than SBR.

Both SBR and NR showed a moderate increase of its resistance to crack opening after being moderately stretch in the direction of crack opening. The significant material softening observed when preconditioning the samples did not affect its mode I fracture toughness. Moreover, large strain preconditioning does not impact noticeably the strain energy release rate. As for the Mullins damage undergone in other directions than the stretching direction during prestraining, that renders the material anisotropic, it also seems to have little impact on the critical strain energy release rate in mode I. The

In order to extend the current analysis, it would be interesting to apply compression and multiaxial prestraining before testing the material resistance to tear. It would be also interesting to test unfilled samples, since they do not undergo any Mullins softening and could be used as comparison for physical interpretations.

References

[1] Buist, JM (1945) Tear resistance I. Mechanisms of tearing of natural and synthetic rubbers. Rubber Chem Technol 18:486-503.

[2] Cadwell SM, Merrill RA, Sloman CM, Yost FL (1940) Dynamic fatigue life of rubber. Rubber Chem Technol 13:304-315.

[3] Diani J, Brieu M, Vacherand JM (2006) A damage directional constitutive model for Mullins effect with permanent set and induced anisotropy. Eur J Mech A/Solids 25:483-496.

[4] Diani J, Fayolle B, Gilormini P (2009) A review on the Mullins effect. Eur Polym J 45:601-612.

[5] Gabrielle B, Vieyres A, Sanseau O, Vanel L, Long D, Sotta P, Albouy PA (2012) Tear rotation in reinforced natural rubber. Constitutive Models for Rubber VII 221-225. Taylor and Francis Group, London.

[6] Gdoutos EE, Schubel PM, Daniel IM (2004) Determination of critical tearing energy of tyre rubber. Strain 40:110-125.

[7] Gherib S, Chazeau L, Pelletier JM, Satha H (2010) Influence of the filler type on the rupture behavior of filled elastomers. J Appl Polym Sci 118:435-445.

[8] Griffith AA (1921) The phenomena of rupture and flow in solids. Phil Trans Royal Soc London A221:163-198.

[9] Hamed GR (2005) Tearing of vulcanized rubber. Rubber Chem Technol 78:548-553.

[10] Itskov M, Haberstroh E, Ehret A, Vohringer M (2006) Experimental observation of the deformation induced anisotropy of the Mullins effect in rubber. Kautsch Gummi Kunstst 59:93-96.

[11] Lake GJ (1970) Application of fracture mechanics to failure in rubber articles, with particular reference to groove cracking in tyres. Conf. Yied, deformation and fracture of polymers.

[12] Lidley PB (1972) Energy for crack growth in model rubber components. Strain Anal 7:132-140.

[13] Machado G, Chagnon G, Favier D (2012) Induced anisotropy by the Mullins effect in filled silicone rubber. Mech Mater 50:70-80.

[14] Mars W, Fatemi A (2002) A literature survey on fatigue analysis approaches for rubber. Int J Fatigue 24:949-61.

[15] Merckel Y, Brieu M, Diani J, Caillard J (2012) A Mullins softening criterion for general loading conditions. J Mech Phys Solids 60:1257-1264.

[16] Mullins L (1969) Softening of rubber by deformation. Rubber Chem Technol 42:339-362.

[17] Rivlin RS, Thomas AG (1953) Rupture of rubber. I. Characteristic energy for tearing. J Polym Sci 10:291-319.

[18] Thomas AG (1994) The development of fracture mechanics for elastomers. Rubber Chem Technol 67:G50-G60.

[19] Trabelsi S, Albouy PA, Rault J (2003) Effective local deformation in stretched filled rubber. Macromolecules 36:9093-9099.